Radio Science, Volume 34, Number 6, Pages 1461–1473, November–December 1999

A new model for the structure function of integrated water vapor in turbulence

Justin P. Bobak

Remote Sensing Physics Branch, Naval Research Laboratory, Washington, D. C.

Christopher S. Ruf

Department of Electrical Engineering, Pennsylvania State University, University Park

Abstract. Turbulent fluctuation of integrated water vapor in the troposphere is one of the major noise sources in radio interferometry. Processed integrated water vapor estimates from microwave radiometers colocated with interferometers have been used to set bounds on this uncertainty. The bound has been in the form of a calculated structure function, which is a measure of temporal or spatial decorrelation of fluctuations. In this paper a new model is presented for the estimation of the structure function in the absence of radiometer measurements. Using this model, the structure function can be estimated using measurements or estimates of a limited number of meteorological parameters. These parameters include boundary layer depth, surface heat and humidity fluxes, entrainment humidity flux, average virtual potential temperature in the boundary layer, and geostrophic wind speed. These parameters can be found or estimated from radiosonde and surface eddy correlation system data. The model is based on a framework of turbulence meteorology and provides excellent agreement when compared with state-of-the-art atmospheric turbulence simulations. Results of preliminary comparisons with ground truth show some excellent agreement, as well as some problems. The performance of the new model exceeds that of one current model.

1. Introduction

In order to perform the triangulation used for pinpointing celestial objects through radio interferometry, the phase of radio waves propagating from these bodies must be precisely measured over a long baseline, sometimes on a global scale. One of the greatest sources of error in the relative phase calculations is the electrical path delay through the troposphere [*Treuhaft and Lowe*, 1991]. This quantity is extremely variable in both time and space. The variability is due predominantly to the wet tropospheric contribution, that portion arising from atmospheric water vapor [*Elgered*, 1993]. Water vapor is one of the most variable of atmospheric constituents, with local concentrations varying from near 0% to about 4% of the Earth's atmosphere [*Huschke*, 1959]. The columnar-integrated water vapor in the atmosphere can be estimated from water vapor radiometer or Global Positioning System (GPS) data [*Westwater et al.*, 1989; *Rocken et al.*, 1993]. However, atmospheric turbulence causes fluctuations in the wet tropospheric path delay as pockets of air with varying humidity move about in unpredictable fashion. The primary location of this turbulence is a layer located adjacent to the Earth's surface. This layer is called the planetary boundary layer (PBL), and its depth ranges from tens of meters to 1 km or more. The fluctuations have temporal extents ranging from less than 1 s to several minutes and cannot be predicted, only estimated statistically.

Since the fluctuations cannot be predicted, radio astronomers have attempted to put bounds on the variations for the calculation of error budgets. One way this can be done is by colocating a microwave water vapor radiometer with the interferometer. The radiometer data are used to estimate the integrated water vapor (IWV), which is closely related to path delay [*Keihm et al.*, 1995]. Statistics of short-term variations in path delay are calculated and used to estimate these bounds on the variation [*Linfield et al.*, 1996].

One common statistic used for this purpose is the structure function [*Tatarskii*, 1961]. This is a measure of the temporal or spatial decorrelation of a fluctu-

Paper number 1999RS900097.
0048-6604/99/1999RS900097$11.00

ating signal. For a parameter χ the temporal structure function is defined as

$$D_\chi(s) = \langle(\chi(t) - \chi(t+s))^2\rangle, \quad (1)$$

where s is the temporal separation and the angle brackets represent the expectation operator. The structure function of path delay can be directly calculated from processed radiometer data, or, when these data are not available, it can be estimated through evaluation of an existing model. The models that have been used in the past have not always performed adequately [*Treuhaft et al.*, 1995].

In this paper a new model for the structure function of vertically integrated water vapor is presented. This model is tied more closely to a meteorological framework than were previous models. For this reason, it requires more geophysical parameters as inputs. However, the promise of improved estimates of the structure function compensates for the additional effort required.

Section 2 discusses previous models for the structure function of integrated quantities. Section 3 presents the basic derivation of the new model. Section 4 introduces similarity theory and the large eddy simulation (LES), which are tools used in the model development. It also lists the simulated turbulence data sets available from LES. Section 5 describes the further development and validation of the basic model through the use of similarity and LES results. Section 6 includes preliminary ground truth comparisons. Additional comparisons with a currently used model are also included. Conclusions, comments, and future directions follow in section 7.

2. Previous Modeling

Much of the previous modeling of the effects of turbulence on integrated quantities has been based on the pioneering work of *Tatarskii* [1961]. Tatarskii derived a structure function model for a quantity in a locally isotropic turbulence field. The PBL is not isotropic except on the smallest scales. However, this assumption greatly simplifies the problem, and it has been used in the majority of the previous work.

In the case of an isotropic field, many quantities have an associated structure function that has a power law form for some range of separation,

$$D_\chi(s) \propto s^\beta, \qquad s_L \ll s \ll s_U, \quad (2)$$

where s_L and s_U are lower and upper limits on the separations for which (2) is valid. During the 1980s, several experiments were conducted in attempts to test the validity of this form when applied to integrated quantities and to find a value for the exponent, β [*Armstrong and Sramek*, 1982; *Bieging et al.*, 1984; *Kasuga et al.*, 1986]. *Treuhaft and Lanyi* [1987] published a model for the structure function of path delay. This model was based on the concept of isotropic turbulence occupying a slab boundary layer. The derived structure function of path delay was a power law form, with an exponent that was a function of the horizontal spatial separation normalized by the depth of the modeled boundary layer. Modifications to this model were published by *Treuhaft et al.* [1995]. These modifications were necessitated by the inability of the earlier model to account for observed turbulence signatures in a new infrared data set. The new model was a two-layer slab and had structure constants (the proportionality constant in equation (2)) that varied with height. Several other improvements were also made to the 1987 model. However, despite best efforts to model the new data, errors of as large as 50% were still present.

Coulman and Vernin [1991] reviewed and reanalyzed the results of *Armstrong and Sramek* [1982], *Treuhaft and Lanyi* [1987], and others and added other, previously unpublished results from Sramek. The reanalysis resulted in a proposed model for the structure function that was similar to that proposed by *Treuhaft and Lanyi* [1987] but with some modifications based on meteorological understanding of turbulent fields.

3. Derivation of the New Model

Because of the large errors in the previous models, the need for a new model was evident. This model was developed on a framework of turbulence meteorology and was supplemented, where necessary, with new empirical results. Its evaluation provides an estimate of the structure function of vertically integrated water vapor. These results can be easily modified to provide structure functions of path delay. The development was performed in terms of integrated water vapor to simplify the use of this model in some recent studies by the authors. These studies have used the structure function of integrated water vapor as a tool for probing the atmosphere [*Bobak and Ruf*, 1996; *Ruf and Beus*, 1997].

The structure function of integrated water vapor was derived as a function of water vapor mixing ratio. The model derivation is straightforward, and the

details can be found in Appendix A. With the assumption that the mean value of the mixing ratio is only a function of altitude, and the further assumption that the turbulent motions can be treated as wide-sense stationary processes, the structure function resulting from the derivation in Appendix A is

$$D_{\mathrm{IWV}}(\tau) = 2A^2 \int_0^\infty \int_0^\infty \exp\left(\frac{-z-z'}{H_1}\right) \cdot \{\langle b'(z,t)b'(z',t)\rangle - \langle b'(z,t)b'(z',t-\tau)\rangle\}\, dz\, dz', \quad (3)$$

where

D_{IWV} structure function of integrated water vapor, cm^2;
τ temporal separation, s;
A constant (see Appendix A);
H_1 dry-air density scale height, m;
$b'(z, t)$ fluctuating component of water vapor mixing ratio at height z and time t, g kg^{-1}.

From (3) the structure function is directly related to the rate at which the correlation between fluctuations at two different heights (z and z') decreases. The structure function includes contributions from all combinations of z and z'. The exponential term and the coefficient outside of the integrals are necessary to convert the integrated mixing ratio correlations into an integrated water vapor structure function. The upper limits on the integration are effectively a small multiple (greater than unity) of the boundary layer depth. Otherwise, (3) is similar in form to the model of *Treuhaft and Lanyi* [1987]. Above the PBL, laminar flow is assumed, resulting in no additional contribution. However, the top of the PBL is not well defined due to entrainment and other processes, so turbulent motions exist above the nominal top of the boundary layer, to additional heights of a few tens of percent of the PBL depth.

Unfortunately, the behavior of point-to-point correlations, like those in (3), has not been studied adequately. Empirical forms for these quantities were developed to enable the evaluation of the model. Before these forms are presented, however, some tools from turbulence research must be mentioned.

4. Tools

4.1. Similarity Theory

Similarity theory is a powerful method for estimating profiles of parameter variances, parameter means, and stresses in a turbulent boundary layer based upon equations involving the correct combinations of geophysical parameters. It was used in the development of a mathematical form for the correlations of mixing ratio fluctuations in (3). A thorough discussion of the background and application of similarity theory is presented by *Stull* [1988].

4.2. Large Eddy Simulation

4.2.1. Description. The large eddy simulation (LES) is a numerical solution of the equations of turbulent fluid motion on a three-dimensional grid [*Moeng*, 1984]. The extreme differences in sizes between the largest and the smallest eddies in the PBL (dimensions range over about 7 orders of magnitude) make it impossible to simulate all eddy sizes. In LES, as the name implies, the large eddies are explicitly included, while the effects of the smaller eddies are implicitly included through modeling.

LES was originally designed for low Reynolds number flows. As such, its application to the high Reynolds number flows in the atmosphere has been questioned. Additional potential problems arise due to the need to rely on models for estimating the effects of small, unmodeled eddies. *Ferziger* [1996] discusses these and other issues in greater detail. Despite these questions, LES is currently the best model available for simulating atmospheric turbulence and the only option for calculating information with the fine resolution necessary.

4.2.2. LES data sets. Readily available LES results were used. Seven of the sets of conditions (cases) were judged to be useful. These cases were mostly representative of convective (unstable) boundary layers, though many were only marginally unstable, and two were neutral. Highly convective boundary layers are characteristic of sunny days over land, while neutral or weakly convective boundary layers are more common over bodies of water or during night hours over land. In these cases the turbulence arises more from a shearing action of faster winds above the PBL. Four of the seven cases included capping temperature inversions on the boundary layers. Unfortunately, only one case included baroclinic conditions, which are distinguished by the presence of a horizontal pressure gradient that is a function of height. These conditions are common in the atmosphere.

The naming convention for these case results is "*Qqqxxxx*." The surface heat flux (in K cm s^{-1}) is given by "*qq*." Larger values represent more highly convective conditions. The presence of either a tem-

Table 1. General Description of Large Eddy Simulation Cases

Name	Highly Convective	Mix of Convection and Shear	Shear Only	Capping Inversion Present
Q24CAP	×			×
Q05CAP		×		×
Q03CAP		×		×
Q03BARO		×		×
Q00CAP			×	×
Q05NOCAP		×		
Q00NOCAP			×	

perature inversion or baroclinic conditions, or the lack of these, is reflected by "*xxxxx*." CAP indicates the presence of a capping inversion, NOCAP indicates no inversion, and BARO indicates the one case that included baroclinic conditions. This last case also included a temperature inversion. Table 1 lists the LES cases used.

5. Model Development

5.1. LES Validation of Equation (3)

In order to test the validity of (3), structure functions of integrated water vapor were calculated from LES information in two ways. The first represented the structure function calculated from water vapor radiometer data by simply substituting estimated integrated water vapor into (1). The second way was by direct evaluation of (3). Figure 1 shows the two structure functions from Q24CAP, the highly convective case. The fit of (3) to the "true" structure function is excellent.

5.2. Developing Forms for the Terms in Equation (3)

Similarity theory can be used to estimate various quantities in turbulence fields. However, no appropriate similarity forms for two-point correlations, such as those in (3), were available. This problem was solved by rewriting the correlations as the product of a correlation coefficient and two standard deviation terms:

$$\langle b'(\psi)b'(\zeta)\rangle = r_{b'b'}(\psi, \zeta)\sigma_{b'}(\psi)\sigma_{b'}(\zeta), \qquad (4)$$

where $r_{b'b'}(\psi, \zeta)$ is the correlation coefficient, $-1 \leq r_{b'b'}(\psi, \zeta) \leq 1$, and $\sigma_{b'}(\psi)$ is the standard deviation of b' at (ψ). In this equation and those that follow, ψ and ζ indicate general argument of the function or operator that precedes them.

5.2.1. Standard deviation of fluctuations. Similarity can be used to evaluate the standard deviation terms. The particular form used in this paper was developed by *Moeng and Wyngaard* [1984]. Their formulation (their equations 3.4 and 3.6) were applied without modification to the current problem.

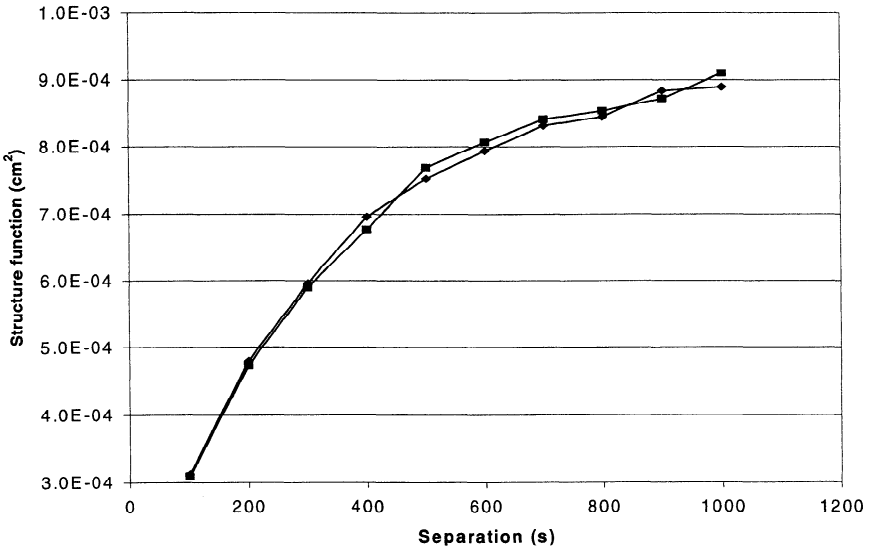

Figure 1. Comparison of structure functions. The points denoted by squares are simulated radiometer-derived values, while points represented by diamonds are calculated from equation (3).

Evaluation requires values for surface humidity flux, entrainment humidity flux, convective velocity, and boundary layer depth. Definitions and descriptions of these inputs are given in Appendix B.

The resulting profiles of standard deviations were compared with statistical profiles from LES, with these latter profiles being treated as "ground truth." Generally, better agreement was found in cases characterized by the presence of capping inversions and high convection. The one baroclinic case available exhibited substandard agreement. Specific examples of behavior are given by *Bobak* [1998].

5.2.2. Correlation coefficient. Using LES results, an empirical form for the correlation coefficient, based on similarity theory, was developed. The details are given by *Bobak* [1998]. Briefly, strong vertical symmetry was noted in the behavior, so the coefficient was made a function of the separation between the two heights, z and z'. In similarity theory, all quantities must be normalized, so the separation was normalized by the boundary layer depth z_i. The time separation τ was normalized by a term related to atmospheric stability [*Willis and Deardorff*, 1976]. The resulting scaling is

$$r(z, z', 0) \propto \frac{|z - z'|}{z_i}, \qquad \tau \frac{U_g}{z_i}, \tag{5}$$

where U_g is the geostrophic wind speed, which is approximately equivalent to the wind speed above the PBL. The correlation coefficients show a logarithmic form as a function of increasing spatial separation. A log linear fit was performed for each time separation of each LES case, resulting in the following estimate of the correlation coefficient:

$$\log_{10}\left(r\left(\frac{|z1 - z2|}{z_i}, \frac{\tau U_g}{z_i}\right)\right) = M\left(\frac{\tau U_g}{z_i}\right)\frac{|z1 - z2|}{z_i} + B\left(\frac{\tau U_g}{z_i}\right), \tag{6}$$

where $M(\zeta) = -0.0362(\zeta)^2 + 0.3456(\zeta) - 0.8355$ and $B(\zeta) = -0.1945(\zeta) - 0.024$.

5.2.3. Entrainment zone correction. Turbulent motions exist well above z_i. Because of the mixture of turbulent and laminar air, this region is difficult to model, and no similarity forms exist for altitudes greater than z_i. However, fluctuations at these heights contribute significantly to the structure function and must be included. A formulation was created to account for the effects of these fluctuations in an ad hoc manner, but a need exists for a framework for more rigorous modeling of parameters at heights above z_i.

An empirical fit to the total error, rather than just that portion of the error which could be traced exactly and exclusively to the water vapor at heights above z_i, was calculated. A large source of error below z_i is the entrainment humidity flux value used in the evaluation of (4). Since this value is connected to the entrainment zone, it was felt that fitting the total error was justified. The details of the development are presented by *Bobak* [1998]. The correction is a fit of the magnitude and time separation behavior of the error to geophysical parameters. Unfortunately, because of limitations in the available LES results, part of the correction is based on only two of the seven available simulations. These were Q24CAP and Q05NOCAP (see Table 1). The resulting correction term, designed to fit the behavior as a function of time separation, is

$$\text{term1} = -0.0245s^2 + 0.2645s + 0.7512, \; s = \frac{\tau z_i}{U_g}. \tag{7}$$

The second portion of the correction, designed to fit the magnitude of the error to geophysical conditions, used results of four LES cases. These cases were Q24CAP, Q05NOCAP, Q03CAP, and Q05CAP. The best fit occurred between error and entrainment humidity flux scale, b_{1^*}. The fit is

$$\text{term2} = 1.5868b_{1^*} + 0.1277. \tag{8}$$

The completely empirical fit based on a small number of points is of concern, and this is considered to be one of the weaker parts of the model. There is a need for a generally improved understanding of entrainment zone processes in the turbulence community.

Equation (3) is normalized by the product of these two correction terms to get the final estimate of the structure function,

$$D_{\text{IWV}}(\tau) = \frac{D'_{\text{IWV}}(\tau)}{\text{term1} \times \text{term2}}, \tag{9}$$

where $D'_{\text{IWV}}(\tau)$ is the estimate of the structure function arising from (3).

5.3. LES Validation of the Full Model

The ratios of structure function values estimated from the forward model to those calculated directly

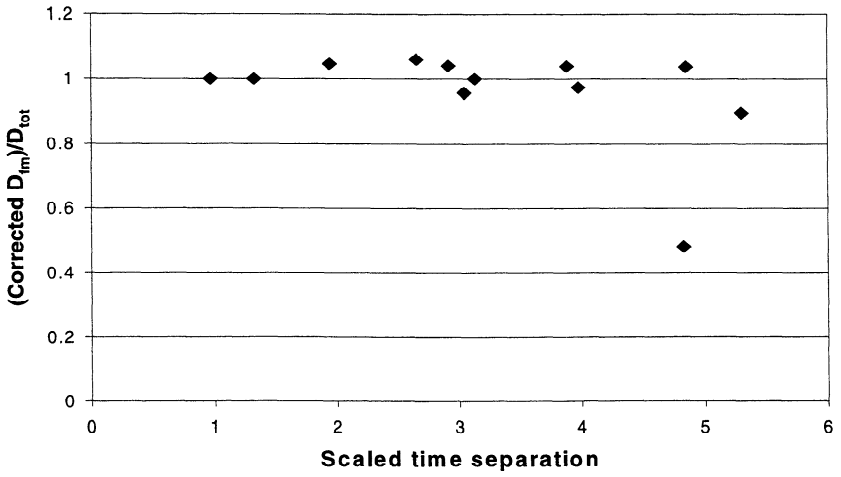

Figure 2. The ratio of the structure function calculated from the forward model (including the correction factor (corrected D_{fm}) to the "true" structure function (D_{tot}) calculated from large eddy simulation (LES) mixing ratio fields. The corrected forward model provides accurate values with little scatter. Outlier is from Q03BARO.

from LES results are shown in Figure 2. The one outlier is from the baroclinic case, which has been discussed as a problem previously. Neglecting this particular point, the average value of the ratio is 1.0, and the standard deviation is 5%. The structure function magnitudes vary over at least an order of magnitude due to the varying atmospheric conditions represented in the LES cases. The new model is estimating the correct value with no bias. A wide range of unstable atmospheric conditions is represented by these points, and the new model performs well under each set of conditions when compared with LES results.

6. Ground Truth Comparison

The new model shows promise when compared with the results of LES. Some preliminary comparisons between true ground truth structure functions and model results were also done. For these purposes, the geophysical parameters necessary for evaluation of the model were taken directly or estimated from measurements.

6.1. Available Data

Archived data from the U.S. Department of Energy's Atmospheric Radiation Measurement Program cloud and radiation test bed in Oklahoma were used for the comparison. Concurrent and colocated data from a ground-based water vapor radiometer, radiosondes, and an eddy correlation flux measurement system were sufficient for this comparison. The data used in the comparisons are from April 1998.

6.1.1. Water vapor radiometer. Estimates of vertically integrated water vapor and cloud liquid were available with a 20-s sampling interval. The cloud liquid data were used to screen for clouds. The forward model was developed using cloud-free conditions, and for this preliminary comparison, cloud-free conditions were most desirable in order to better gauge the performance of the model. The integrated water vapor data were used to calculate the ground truth structure function normally.

6.1.2. Radiosondes. Data from radiosonde launches provided the bulk of the inputs to the forward model. Profiles of virtual potential temperature, Θ_v, were calculated from air temperature, air pressure, and relative humidity. From the Θ_v profiles, the boundary layer depth was estimated. The geostrophic wind speed U_g was also estimated by the first measured wind speed above z_i.

Radiosondes are a relatively inexpensive and readily available source for several of the needed inputs, but they are not ideal. They provide only a snapshot of the turbulent boundary layer, when what is desired is statistical information. Radar wind profiling systems and/or radio acoustic sounding systems may provide better data. However, lack of sufficient concurrent data prohibited the use of data from such instruments in this initial analysis.

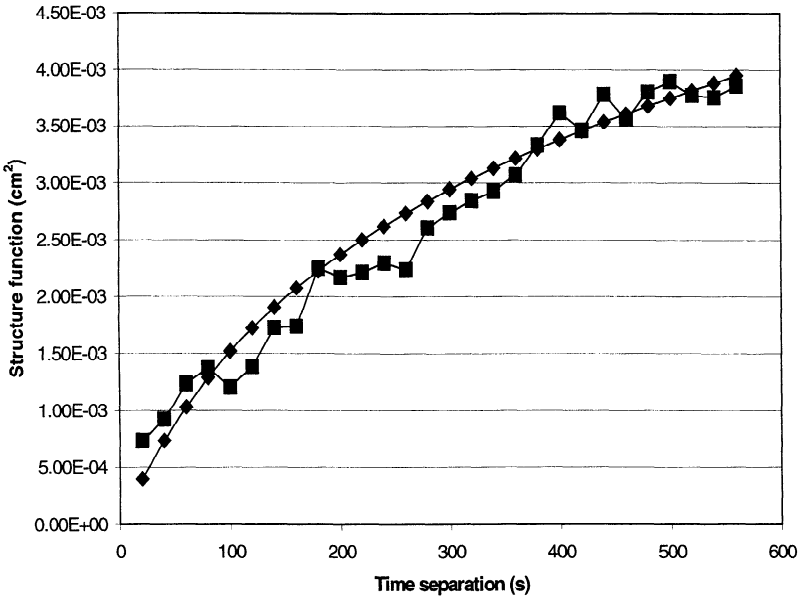

Figure 3. An example of a good fit between the forward model estimate of the structure function (diamonds) and the ground truth structure function. Data are from April 7.

6.1.3. Eddy correlation flux measurement system. The eddy correlation flux measurement system (ECOR) consists of a three-dimensional sonic anemometer and an infrared hygrometer. This system provided surface temperature flux and surface humidity flux.

There was no good way to measure entrainment humidity flux, which is a necessary component for the evaluation of the forward model. Entrainment temperature flux can be roughly estimated as 20% of the magnitude of surface temperature flux [*Stull*, 1988]. Using this as a guideline, entrainment humidity flux values with magnitudes that were 20% of the surface humidity flux values were used. The resulting structure functions consistently underestimated the ground truth structure functions. Also, LES results included surface and entrainment humidity fluxes of approximately equal magnitude. Estimating the magnitude of the entrainment humidity flux by 100% of the surface humidity flux provided much better structure function estimates, and these estimates were used in the results in this section.

6.2. Ground Truth Comparison Results

Data taken during afternoon (about 1300–1500 LT) were used for comparison, as the convective PBL is most fully developed during this time of the day. There are 14 data points with simultaneous data from the three necessary sources (ECOR, water vapor radiometer (WVR), and radiosonde observation (Raob)) and with no significant cloud cover.

About one third of the points display excellent agreement between forward model estimates and ground truth. An example is shown in Figure 3. As can be seen, both the absolute value and slope (time dependence) are in extremely good agreement.

A further third of the points show a lesser degree of agreement. One example is shown in Figure 4. In this particular case, the magnitude has varying degrees of agreement, but the slope is not in good agreement with ground truth. Other cases in this category demonstrate the opposite behavior, with the slopes in fairly good agreement but with errors in the magnitudes.

The final third of the points are characterized by disappointing fits. An example is shown in Figure 5. The model badly overestimates the magnitude in some cases and badly underestimates it in others.

6.3. Comparison With *Treuhaft and Lanyi*'s [1987] Model

In order to compare the performance of the new model to that of a currently used model [*Linfield et al.*, 1996], *Treuhaft and Lanyi*'s [1987] model was modified to estimate the structure function of integrated water vapor rather than path delay. The details of this modification are presented in Appendix C. The

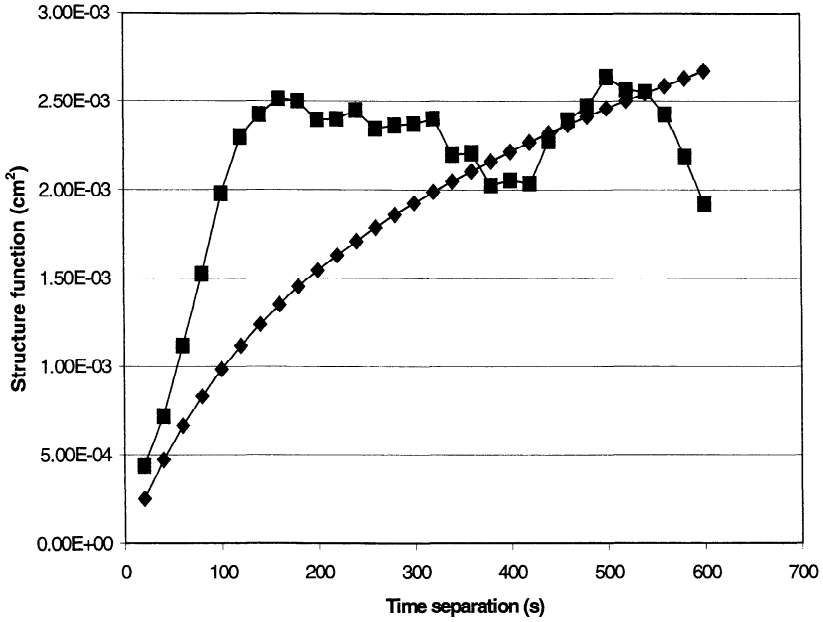

Figure 4. The April 6 case comparison shows fair agreement between the forward model output (diamonds) and ground truth.

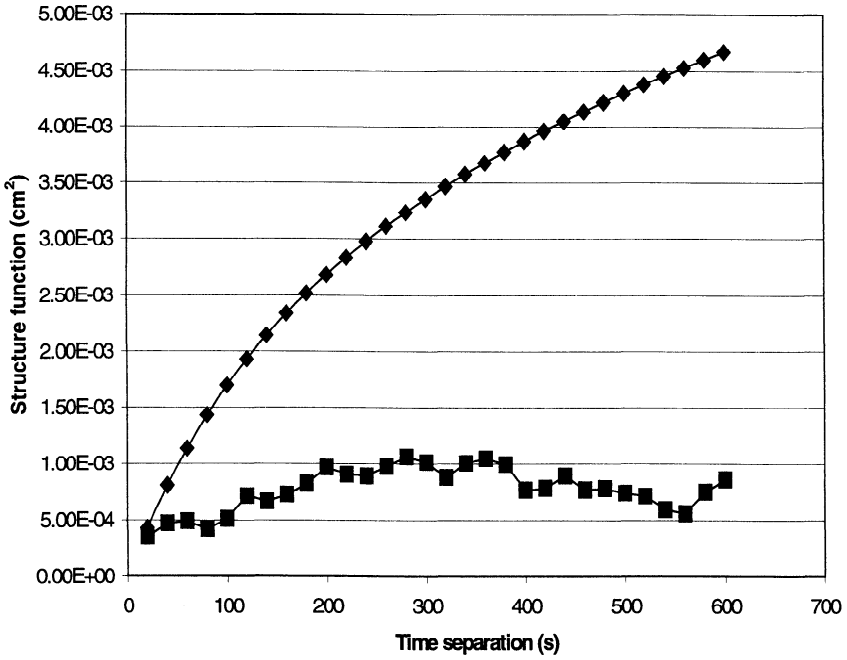

Figure 5. An example of a poor fit with ground truth data from April 9. The forward model output is represented by diamonds.

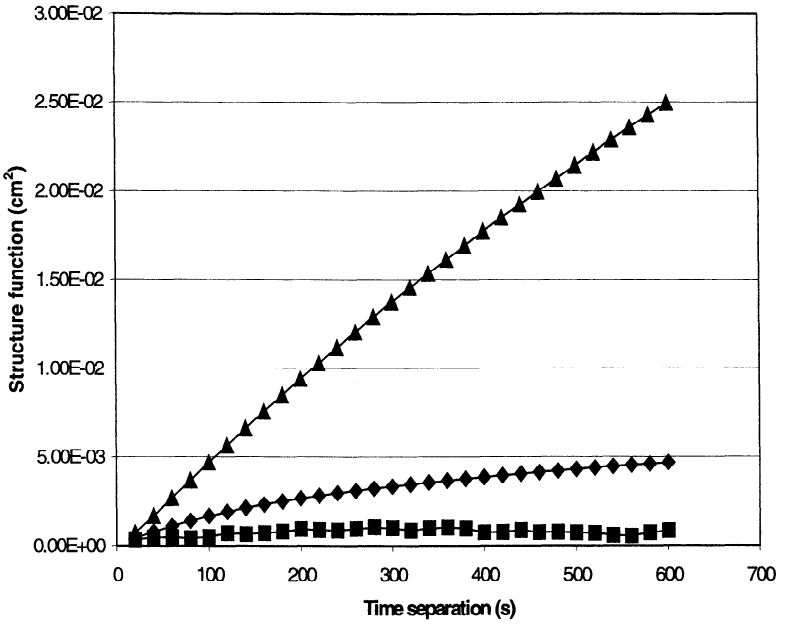

Figure 6. Comparison of results from another model. *Treuhaft and Lanyi*'s [1987] model (triangles), modified as discussed in Appendix C, overestimates the ground truth (squares). The new forward model (diamonds) shows a better fit than the other model. The ground truth data are the same as those shown in Figure 5.

comparison was done for the data points shown in Figures 3, 4, and 5. An example is shown in Figure 6, using the same ground truth data as in Figure 5. The Treuhaft and Lanyi model overestimates the ground truth. The new forward model is an improvement, even in this case, which is one of the poorly performing cases. In each of the three cases tested the new model predicts the measured structure function with significantly better accuracy than does the Treuhaft and Lanyi model.

7. Discussion and Conclusions

The need to estimate the structure function of integrated water vapor for radio interferometry has been discussed, and a description of some past modeling efforts has been given. The development of the new model was detailed. The pertinent geophysical inputs are the depth of the boundary layer, the convective velocity, the geostrophic wind speed, the surface humidity flux, and the entrainment humidity flux. The first four of these quantities can be provided by radiosondes and an eddy correlation system. In comparisons with ground truth, the last quantity was estimated with some success from the value for surface humidity flux.

Several potential limitations in the development of the new model must be kept in mind. The large eddy simulation cases used to develop and test the model were mostly representative of convective (unstable) boundary layers, though some of them were only marginally unstable. More LES cases are needed in order to apply these results to stable atmospheres. Also, baroclinic conditions, which are very common in the atmosphere, were not well represented in the LES cases on hand. Judging from the one case that was available, the model may have difficulty dealing with this atmospheric condition. The model is currently limited to scaled time separations, s, of about 5 or less. This means that the product of time separation and mean wind speed should be less than 5 times the depth of the boundary layer. Also, the correction for entrainment zone effects suffers from the current lack of modeling for entrainment processes.

Keeping these limitations in mind, model validation against LES cases was excellent. This should not be surprising since some of these same LES cases provided the empirical correction used for the entrainment zone. The one glaring potential problem was the single baroclinic case.

A more illuminating test was the comparison of

forward model estimates with ground truth from the cloud and radiation test bed site in Oklahoma. Some of the fits were excellent. This was better than expected when potential problems such as the entrainment zone correction, the lack of baroclinic conditions in the model development, and the need to use radiosonde samples rather than statistics of the atmosphere were considered. The ground truth comparisons show the great potential of the new model. In addition, they demonstrate that the model can be evaluated with a minimum of ground instrumentation.

The fits judged to be excellent, fair, or poor tended to group together, with periods of a few days. This may suggest a possible correlation with frontal movement. However, no connection between any geophysical parameter and the quality of the model performance could be found in this preliminary assessment.

The new model was shown to outperform a currently used model for three different cases. This was true even in the case where the new model performed poorly compared with ground truth. This suggests that the additional work and instrumentation needed for evaluating the new model are worthwhile in many situations.

As the next step, a more extensive database needs to be assembled in order to first isolate the mechanism responsible for the poor performance of the model during some periods. If possible, this poor performance will be corrected, or at least predicted. Finally, the set of conditions under which the model performs well should be better delineated and expanded, if possible, to include stable conditions, baroclinic conditions, and cloudy conditions.

Appendix A: Derivation of the New Model

An outline of the mathematical development of the model is presented here. For more details, see *Bobak* [1998].

The total water vapor mixing ratio is represented by

$$\tilde{b}(x, y, z, t) = B(x, y, z, t) + b'(x, y, z, t)$$

$$\langle \tilde{b}(x, y, z, t) \rangle = B(x, y, z, t) \tag{A1}$$

$$\langle b'(x, y, z, t) \rangle = 0,$$

where the first term on the right side of the first equation is the mean value of mixing ratio, and the second term on the right represents turbulent fluctuations about this mean. By multiplying the mixing ratio by the density of other atmospheric constituents, the density of water vapor can be calculated. An equation for estimating the density of other constituents is given by *Ulaby et al.* [1981] as

$$\rho_{\text{dry}}(z) = 1.225 \exp\left(\frac{-z}{H_1}\right), \tag{A2}$$

where $\rho_{\text{dry}}(z)$ is the density of dry air at height z, kg m^{-3}; z is altitude, in meters; and H_1 is density scale height, 9500 m for U.S. Standard Atmosphere (1962).

Multiplication gives the water vapor density at height z:

$$\tilde{\rho}_v(x, y, z, t) = \tilde{b}(x, y, z, t)\rho_{\text{dry}}(z), \tag{A3}$$

where $\tilde{\rho}_v(x, y, z, t)$ is water vapor density, g m^{-3}, and $\tilde{b}(x, y, z, t)$ is water vapor mixing ratio, g kg^{-1}. Integrating this product over the vertical extent of the atmosphere gives the integrated water vapor:

$$\text{IWV}(x, y, t) = 10^{-4} \int_0^\infty \tilde{\rho}_v(x, y, z, t)\, dz, \tag{A4}$$

where IWV(x, y, t) is integrated water vapor, in centimeters.

The factor of 10^{-4} arises from the conversion of units to centimeters of integrated water vapor. The time separation structure function is derived here, and the conversion to a spatial separation structure function is straightforward.

IWV can be rewritten using (A2) and (A3) as

$$\text{IWV}(x, y, t) = A \int_0^\infty \exp\left(\frac{-z}{H_1}\right) \tilde{b}(x, y, z, t)\, dz, \tag{A5}$$

where $A = 1.225 \times 10^{-4}$ for IWV, in centimeters; mixing ratio is in g kg^{-1}; and z is in meters. Using this result and following the definition of the structure function,

$$\begin{aligned} D_{\text{IWV}}(x,y,t,t-\tau) &\equiv \langle (\text{IWV}(x,y,t) - \text{IWV}(x,y,t-\tau))^2 \rangle \\ &= A^2 \int_0^\infty \int_0^\infty \exp\left(\frac{-z-z'}{H_1}\right) \{ \langle \tilde{b}(x, y, z, t)\tilde{b}(x, y, z', t) \rangle \\ &\quad - \langle \tilde{b}(x, y, z, t)\tilde{b}(x, y, z', t-\tau) \rangle \\ &\quad - \langle \tilde{b}(x, y, z, t-\tau)\tilde{b}(x, y, z', t) \rangle \\ &\quad + \langle \tilde{b}(x, y, z, t-\tau)\tilde{b}(x, y, z', t-\tau) \rangle \} \, dz\, dz'. \end{aligned} \tag{A6}$$

The mean mixing ratio B is assumed to be a function only of the spatial coordinate z by assumption of

horizontal homogeneity and of steady state behavior. Then (A1) becomes

$$\tilde{b}(x, y, z, t) = B(z) + b'(x, y, z, t). \quad \text{(A7)}$$

Using $\langle b' \rangle = 0$ and $\langle B \rangle = B$ from (A1), the terms of the form $\langle \tilde{b}(\psi)\tilde{b}(\zeta) \rangle$ can be rewritten as

$$\langle \tilde{b}(\psi)\tilde{b}(\zeta) \rangle = B(\psi)B(\zeta) + \langle b'(\psi)b'(\zeta) \rangle. \quad \text{(A8)}$$

Substituting this result into (A6) gives

$$D_{\mathrm{IWV}}(x, y, t, t - \tau) = A^2 \int_0^\infty \int_0^\infty \exp\left(\frac{-z - z'}{H_1}\right)$$
$$\cdot \{\langle b'(x, y, z, t)b'(x, y, z', t) \rangle$$
$$- \langle b'(x, y, z, t)b'(x, y, z', t - \tau) \rangle$$
$$- \langle b'(x, y, z, t - \tau)b'(x, y, z', t) \rangle$$
$$+ \langle b'(x, y, z, t - \tau)b'(x, y, z', t - \tau) \rangle\} \, dz \, dz'. \quad \text{(A9)}$$

With the assumption that only the time separation matters, (A9) becomes

$$D_{\mathrm{IWV}}(x, y, \tau) = 2A^2 \int_0^\infty \int_0^\infty \exp\left(\frac{-z - z'}{H_1}\right)$$
$$\cdot \{\langle b'(x, y, z, t)b'(x, y, z', t) \rangle$$
$$- \langle b'(x, y, z, t)b'(x, y, z', t - \tau) \rangle\} \, dz \, dz'. \quad \text{(A10)}$$

In practice, the ensemble average represented by the expectation operator will be replaced by a spatial (horizontal) average, in which case the x and y dependence is suppressed and

$$D_{\mathrm{IWV}}(\tau) = 2A^2 \int_0^\infty \int_0^\infty \exp\left(\frac{-z - z'}{H_1}\right)$$
$$\cdot \{\langle b'(z, t)b'(z', t) \rangle - \langle b'(z, t)b'(z', t - \tau) \rangle\} \, dz \, dz'. \quad \text{(A11)}$$

Appendix B: Definitions of Needed Turbulent Quantities

There are several definitions for the boundary layer depth, z_i. In practice, the first vertical point at which the virtual potential temperature (a measure of air parcel buoyancy) changed by more than a few tenths of a kelvin from the boundary layer average value was chosen as z_i. For more discussion, see *Stull* [1988]. The virtual potential temperature is defined as [*Stull*, 1988]

$$\theta_v = T\left(\frac{P_o}{P}\right)^{0.286}(1 + 0.61b), \quad \text{(B1)}$$

where T is the air temperature, P is the air pressure, b is the water vapor mixing ratio (g g^{-1}) at the altitude of θ_v, and P_o is the surface air pressure.

The surface humidity flux scale and entrainment humidity flux scale are defined as

$$b_{*0} = \frac{\langle w'b' \rangle_s}{w_*} \quad \text{(B2)}$$

$$b_{*1} = \frac{\langle w'b' \rangle_{zi}}{w_*}, \quad \text{(B3)}$$

respectively. They are defined in terms of the parameters w' = fluctuations in vertical wind speed, m s^{-1}; b' = scalar fluctuations, g kg^{-1}, for water vapor mixing ratio; and [*Stull*, 1988]

$$w_* = \left(\frac{g}{\Theta_v}\langle w'\theta_v' \rangle_s z_i\right)^{1/3}. \quad \text{(B4)}$$

The last quantity is called the convective velocity and is a characteristic speed of vertical motion in the turbulent field. It is defined in terms of

- g gravitational acceleration, m s^{-2};
- Θ_v average virtual potential temperature, K;
- θ_v' fluctuations in the virtual potential temperature, K;
- z_i boundary layer depth, m.

In the above equations, $\langle \ \rangle_s$ refers to the expectation of values at the surface, while $\langle \ \rangle_{zi}$ refers to expectation of values at the top of the boundary layer, z_i.

The estimate for the entrainment humidity flux scale that was used in the comparisons of the forward model to ground truth was

$$b_{*1} \cong b_{*0}. \quad \text{(B5)}$$

Appendix C: Modifying the *Treuhaft and Lanyi* [1987] Model to Estimate Integrated Water Vapor Structure Functions

The *Treuhaft and Lanyi* [1987] model (hereinafter referred to as TL87) was developed to estimate the structure function of path delay. In order to compare it with the new model, TL87 was modified to estimate the structure function of integrated water vapor, in the following manner:

For a zenith path, equation 5 from TL87 becomes

$$D_\tau(\rho) = \int_0^h \int_0^h \{D_\chi([\rho^2 + (z - z')^2]^{1/2}) - D_\chi(|z - z'|)\}\, dz\, dz'. \tag{C1}$$

Following the steps in Appendix A, this can be rewritten as the structure function of integrated water vapor as

$$D_{\mathrm{IWV}}(\rho) = A^2 \int_0^{zi} \int_0^{zi} \exp\left(\frac{-z - z'}{H_1}\right) \cdot \{D_b([\rho^2 + (z - z')^2]^{1/2}) - D_b(|z - z'|)\}\, dz\, dz', \tag{C2}$$

where $A = 1.225 \times 10^{-4}$ (see Appendix A), $H_1 = 9500$ m is the scale height of air density, and $D_b(r) = C_b^2 r^{2/3}$ is the structure function of water vapor mixing ratio fluctuations. This definition of $D_b(r)$ is analogous to that used for refractivity by TL87. The use of Taylor's hypothesis [*Taylor*, 1938], by which the motion of turbulent structures has been treated as a "frozen flow" pushed by the prevailing winds, is used by TL87, so the conversion

$$\rho = Ut, \tag{C3}$$

where U is the prevailing wind in the boundary layer and t is the time separation, will be made. Both surface and boundary layer average values for U were tested, with the surface wind providing a more accurate ultimate estimate of structure function when (C2) was ultimately evaluated. Equation (C2) can be evaluated if a value for C_b^2, the structure parameter for water vapor mixing ratio fluctuations, can be found. The first step is to write out the definition of this structure function,

$$D_b = \langle (b_1 - b_2)^2 \rangle, \tag{C4}$$

where b is water vapor mixing ratio, in kg kg^{-1}. The mixing ratio can be rewritten in terms of vapor pressure [*McIntosh*, 1972] as

$$b = \frac{\varepsilon e'}{p - e'}, \tag{C5}$$

where $\varepsilon = 0.62197$, p is total air pressure, and e' is water vapor pressure.

Equation (C5) is substituted into (C4), and total air pressure is assumed relatively constant. Realizing that p is about 2 orders of magnitude larger than e',

$$D_b = C_b^2 r^{2/3} \cong \frac{\varepsilon^2}{p^2} \langle (e'_1 - e'_2)^2 \rangle = \frac{\varepsilon^2}{p^2} D_{e'} = \frac{\varepsilon^2}{p^2} C_{e'}^2 r^{2/3}. \tag{C6}$$

From (C6),

$$C_b^2 \cong \frac{\varepsilon^2}{p^2} C_{e'}^2, \tag{C7}$$

when b is in kg kg^{-1} and p is in millibars. To be consistent with the development in Appendix A, b should be in g kg^{-1}, which leads to

$$C_b^2 \cong \left(\frac{1000\varepsilon}{p}\right)^2 C_{e'}^2 \cong 0.5 C_{e'}^2, \tag{C8}$$

with as much accuracy as is warranted when dealing with turbulence. As pointed out by *Coulman and Vernin* [1991], the results of *Wesely* [1976] show that

$$C_{e'}^2 \cong 25 C_T^2 \tag{C9}$$

at microwave frequencies, where C_T^2 is the structure parameter for temperature fluctuations, so that

$$C_b^2 \cong \frac{25}{2} C_T^2 \tag{C10}$$

with b in g kg^{-1}. *Wyngaard et al.* [1971] gives a similarity form for C_T^2 as

$$C_T^2 = 2.68 \left(\frac{g}{\langle T \rangle}\right)^{-2/3} \left(\frac{z}{\langle w'\theta' \rangle_s}\right)^{-4/3}, \tag{C11}$$

where g is gravitational acceleration, m s^{-2}, and T is air temperature, in kelvins.

Equation (C2) can now be evaluated.

Acknowledgments. Data were obtained from the Atmospheric Radiation Measurement (ARM) Program sponsored by the U.S. Department of Energy, Office of Science, Office of Biological and Environmental Research, Environmental Sciences Division. The efforts of Martin Otte and John Wyngaard in providing LES results are greatly appreciated.

References

Armstrong, J. W., and R. A. Sramek, Observations of tropospheric phase scintillations at 5 GHz on vertical paths, *Radio Sci.*, *17*(6), 1579–1586, 1982.

Bieging, J. H., J. Morgan, W. J. Welch, S. N. Vogel, and M. C. H. Wright, Interferometer measurements of atmospheric phase noise at 86 GHz, *Radio Sci.*, *19*(6), 1505–1509, 1984.

Bobak, J. P., Modeling the effects of turbulence on water vapor radiometer measurements, Ph.D. dissertation, Pa. State Univ., University Park, 1998.

Bobak, J. P., and C. S. Ruf, Prediction of water vapor scale height from integrated water vapor measurements, in *Proceedings of the 1996 International Geoscience and Remote Sensing Symposium*, vol. III, pp. 1692–1694, IEEE Press, Piscataway, N. J., 1996.

Coulman, C. E., and J. Vernin, Significance of anisotropy and the outer scale of turbulence for optical and radio seeing, *Appl. Opt.*, *30*(1), 118–126, 1991.

Elgered, G., Tropospheric radio-path delay from ground-based microwave radiometry, in *Atmospheric Remote Sensing by Microwave Radiometry*, edited by M. A. Janssen, pp. 215–258, John Wiley, New York, 1993.

Ferziger, J. H., Large eddy simulation, in *Simulation and Modeling of Turbulent Flows*, edited by T. Gatski, M. Hussaini, and J. Lumley, pp. 109–154, Oxford Univ. Press, New York, 1996.

Huschke, R. E., *Glossary of Meteorology*, Am. Meteorol. Soc., Boston, Mass., 1959.

Kasuga, T., M. Ishiguro, and R. Kawabe, Interferometric measurement of tropospheric phase fluctuations at 22 GHz on antenna spacings of 27 to 540 m, *IEEE Trans. Antennas Propag.*, *AP-34*(6), 797–803, 1986.

Keihm, S. J., M. A. Janssen, and C. S. Ruf, TOPEX/Poseidon microwave radiometer (TMR), III, Wet troposphere range correction algorithm and pre-launch error budget, *IEEE Trans. Geosci. Remote Sens.*, *33*(1), 147–161, 1995.

Linfield, R. P., S. J. Keihm, L. P. Teitelbaum, S. J. Walter, M. J. Mahoney, R. N. Treuhaft, and L. J. Skjerve, A test of water vapor radiometer–based troposphere calibration using very long baseline interferometry observations on a 21-km baseline, *Radio Sci.*, *31*(1), 129–146, 1996.

McIntosh, D. H., *Meteorological Glossary*, Chem. Publ., New York, 1972.

Moeng, C.-H., A large-eddy-simulation model for the study of planetary boundary-layer turbulence, *J. Atmos. Sci.*, *41*(13), 2052–2062, 1984.

Moeng, C.-H., and J. C. Wyngaard, Statistics of conservative scalars in the convective boundary layer, *J. Atmos. Sci.*, *41*(21), 3161–3169, 1984.

Rocken, C., R. Ware, T. Van Hove, F. Solheim, C. Alber, J. Johnson, M. Bevis, and S. Businger, Sensing atmospheric water vapor with the Global Positioning System, *Geophys. Res. Lett.*, *20*(23), 2631–2634, 1993.

Ruf, C. S., and S. E. Beus, Retrieval of tropospheric water vapor scale height from horizontal turbulence structure, *IEEE Trans. Geosci. Remote Sens.*, *35*(2), 203–211, 1997.

Stull, R. B., *An Introduction to Boundary Layer Meteorology*, Kluwer Acad., Norwell, Mass., 1988.

Tatarskii, V. I., *Wave Propagation in a Turbulent Medium* (translated from the Russian by R. A. Silverman), McGraw-Hill, New York, 1961.

Taylor, G. I., The spectrum of turbulence, *Proc. R. Soc. London, Ser. A*, *CLXIV*, 476–490, Feb. 18, 1938.

Treuhaft, R. N., and G. E. Lanyi, The effect of the dynamic wet troposphere on radio interferometric measurements, *Radio Sci.*, *22*(2), 251–265, 1987.

Treuhaft, R. N., and S. T. Lowe, A measurement of planetary relativistic deflection, *Astron. J.*, *102*(5), 1879–1888, 1991.

Treuhaft, R. N., S. T. Lowe, M. Bester, W. C. Danchi, and C. H. Townes, Vertical scales of turbulence at the Mount Wilson Observatory, *Astrophys. J.*, *453*, 522–531, Nov. 1, 1995.

Ulaby, F. T., R. K. Moore, and A. K. Fung, *Microwave Remote Sensing: Active and Passive*, vol. I, *Microwave Remote Sensing Fundamentals and Radiometry*, Artech House, Norwood, Mass., 1981.

Wesely, M. L., The combined effect of temperature and humidity fluctuations on refractive index, *J. Appl. Meteorol.*, *15*, 43–49, Jan. 1976.

Westwater, E. R., M. J. Falls, and I. A. Popa Fotino, Ground-based microwave radiometric observations of precipitable water vapor: A comparison with ground truth from two radiosonde observing systems, *J. Atmos. Oceanic Technol.*, *6*, 724–730, Aug. 1989.

Willis, G. E., and J. W. Deardorff, On the use of Taylor's translation hypothesis for diffusion in the mixed layer, *Q. J. R. Meteorol. Soc.*, *102*, 817–822, 1976.

Wyngaard, J. C., Y. Izumi, and S. A. Collins Jr., Behavior of the refractive index structure parameter near the ground, *J. Opt. Soc. Am.*, *61*, 1646–1650, 1971.

J. P. Bobak, Remote Sensing Physics Branch, Naval Research Laboratory, 4555 Overlook Avenue SW, Washington, DC 20375. (bobak@vaximg.nrl.navy.mil)

C. S. Ruf, Department of Electrical Engineering, Pennsylvania State University, 323A Electrical Engineering East, University Park, PA 16802.

(Received December 7, 1998; revised August 27, 1999; accepted September 1, 1999.)